6-3-2005

Influence of optical fiber coating damage in the light transmissivity characteristics of microbend sensors

Franz Campero

Paul J. Cosentino

David C. Fleming

Edward H. Kalajian

Barry G. Grossman

Influence of optical fiber coating damage in the light transmissivity characteristics of microbend sensors

Franz Campero[1a] , Paul Cosentino[a], David Fleming[a], Edward Kalajian[a], and Barry Grossman[a]
[a]Florida Institute of Technology, 150 W. University Blvd., Melbourne, FL, USA

ABSTRACT

A laboratory testing and engineering modeling study was completed to determine the influence of fiber optic coating damage caused by microbend contact on the performance of microbend sensors developed based on relatively low cost single-sided microbending technique using a multimode optical fiber. A testing method was designed, developed and implemented to determine the loads that caused optical fiber glass-coating debonding and coating fracture. Finite Element models of the fiber-deformer system were developed to study the failure modes and predict the stresses that caused this failure. Loads and displacements predicted by Finite Element models were found to be in good agreement with load and displacement values observed during the experimental analyses. It was found that optical fiber coating fracture changes the transmissivity output response but does not affect the recovery of the light transmissivity properties of the optical fiber. Viscoelastic effects were found to influence the behavior of the fiber-deformer system. It was also found that glass-coating debonding and coating fracture during a load-unload cycle are major causes of variability and error during microbend sensor calibration.

Keywords: Optical fiber; coating; delamination; fracture; microbending; finite element analysis; Fluortex® ETFE

1. INTRODUCTION

Damage mechanisms such as surface cracks and plastic deformations can significantly reduce the service life and affect the performance of the optical fiber [1, 2]. Therefore, appropriate understandings of the fiber-deformer interaction and the effects caused by contact between optical fiber and deformer are crucial to guarantee a reliable performance of the sensor throughout its service life.

When a microbend sensor is deflected, the light transmitted through the optical fiber decreases. Correlating the loss of light transmissivity with the deflections on the sensor makes possible to determine the magnitude of the measurand. The load/stress transfer mechanism that allows sensing is the contact between optical fiber and deformer.

2. EXPERIMENTAL DESIGN

To analyze the behavior of the optical fiber under contact with a deformer, a "one-strand" microbend sensor was built (Figure 1). The optical fiber lead ends on these one-strand sensors were fitted with Fiber Instrument Sales ST type connectors to allow light to be transmitted. Corning® 50/125/250 multimode optical fiber was used. In order to protect the fiber-connector joints a Kevlar® furcating tube was used. A length of approximately 35 centimeters of optical fiber was left exposed to allow direct contact with the deformer during testing.

Since Fluortex® ETFE mesh was successfully employed in the fabrication of microbend optical fiber sensors, presenting satisfactory results [2, 3], one strand of this material was used as a deformer during this research.

[1] Dr.Franz@gmail.com Phone: (561) 243-4525

Smart Structures and Materials 2005: Sensors and Smart Structures Technologies for Civil, Mechanical, and Aerospace Systems, edited by Masayoshi Tomizuka, Proc. of SPIE Vol. 5765 (SPIE, Bellingham, WA, 2005) · 0277-786X/05/$15 · doi: 10.1117/12.601976

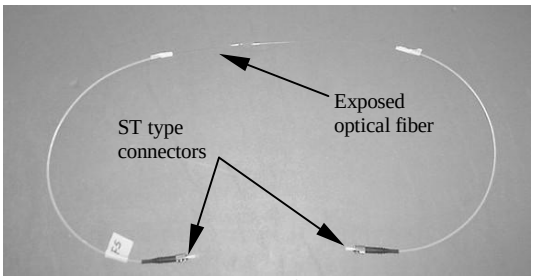

Figure 1. One-strand fiber optic sensor

The one-strand sensor testing methodology adopted simulated what occurs in a microbend sensor. Figure 2 shows a schematic of the mechanical testing conducted. One-strand optical fiber microbend sensor and deformer were placed on an unconfined compression apparatus (Figure 2) with their axes at an approximate angle of 90° and perpendicularly loaded by a monotonically increasing displacement; the speed of the moving platen was kept approximately constant during each test.

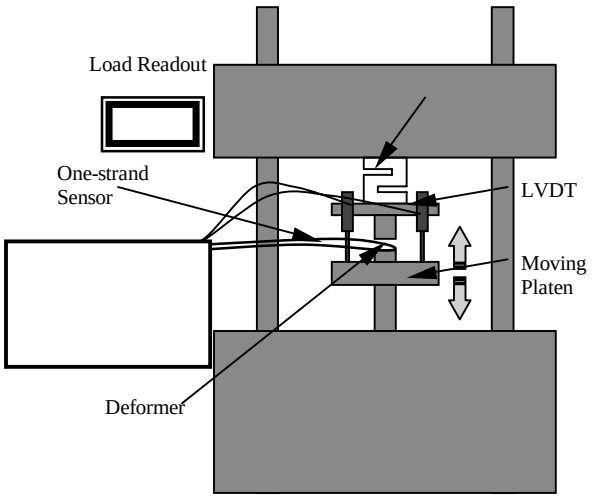

Figure 2. Schematic of fiber-deformer testing

Load, deformation and transmissivity variations were monitored throughout all tests. Transmissivity and deformations were continuously sampled by the data acquisition software every 0.5 seconds yielding between 800 and 2,500 points per test in the optical performance testing curves.

Table 1. Summary of nominal geometric and mechanical properties of the deformer.

Deformer Material	Fluortex® EFTE
Tensile Modulus [MPa]	920 (below 15 MPa) 80 (above 18 MPa)
Compressive Modulus [MPa]	860 (below 12 MPa) 100 (above14 MPa)
Tensile Strength [MPa]	47
Compressive Strength [MPa]	17 (defined at 5 % strain)
Elongation at Break [%] (at 23 °C)	25
Deformer Diameter [μm]	250 ± 10
Poisson's Ratio	N/A
Specific Gravity	1.75

3. MECHANICAL TESTING

To determine the load that caused coating fracture several sets of tests were conducted and halted at different load intervals. Scanning Electron Microscope (SEM) photographs were used to evaluate the first coating crack manifestation.

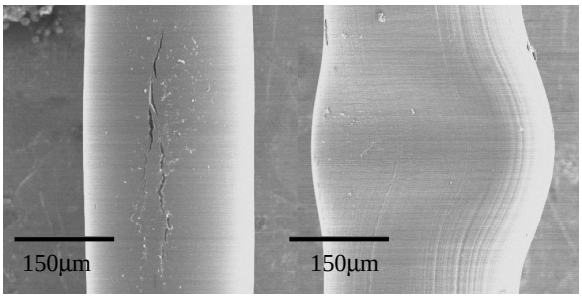

Figure 3. Optical fiber coating first crack manifestations (left). ETFE deformer (right): severe signs of plastic deformation.

Table 2 summarizes the loads and damage nature observed. It should be noted that the load cell had a tolerance of ±3 N.

Table 2. Mechanical testing summary.

Target Load [N]	Actual Load [N]		Remarks
	Test 1	Test 2	
5	5.1	5.1	no signs of damage
10	11.6	9.8	beginning of debonding
20	22.7	20.3	noticeable debonding
30	33.8	31.0	noticeable debonding
40	45.4	43.7	first crack manifestation
60	67.6	65.1	cracking
80	89.0	86.3	cracking

Because the sensitivity of the load cell and the load spacing in the tests it was estimated that coating fracture occurred at loads between 35 and 45 N. Cracks were observed to occur at the point of contact between deformer and optical fiber only. Noticeable glass-coating interface debonding was observed in specimens tested at loads greater than approximately 10 N. Because of the viscoelastic nature of the coatings, the debonding area increased with time.

4. OPTICAL PERFORMANCE TESTING

Although light transmissivity was monitored continuously throughout mechanical testing, conclusions about its behavior could not be drawn because of the nature of the testing (load to a predetermined value and halt the test to study the damage produced by that load). To determine the influence of the damage caused by the different loads (observed during the mechanical testing phase) on the light transmissivity output response, optical performance tests were conducted to loads that permitted a complete development of the transmissivity curves.

A noticeable change of slope in the light transmissivity vs. displacement curves was observed to occur at loads similar to coating fracture loads determined during the mechanical testing phase (between 35 and 45 N). All tests were performed at constant room temperature (23 °C). In an attempt to determine the cause of variability observed in the results, and because temperature and strain rate typically influence the fracture characteristics of materials,

test speed was controlled by carefully monitoring the displacement rate of the moving platen. It was observed that the transmissivity decreased linearly up to about 60 to 70 % where a noticeable change in its curve slope occurred. After this abrupt change of slope, the transmissivity curves continued decreasing linearly with load increments until the test was stopped. Figure 4 presents the load-displacement-transmissivity curves and Table 3 summarizes the results.

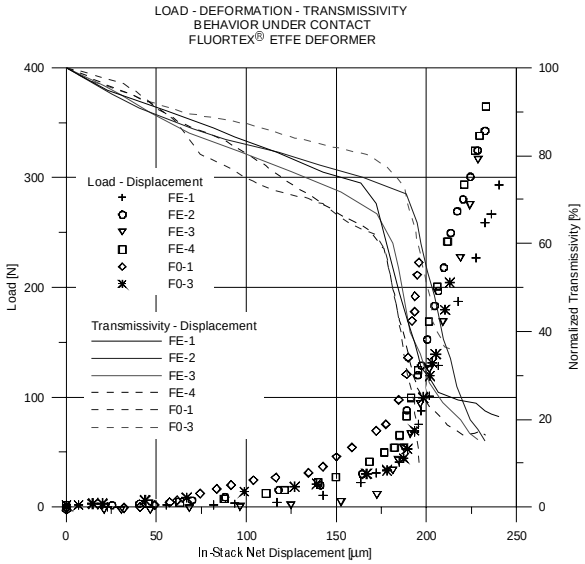

Figure 4. Load-displacement-transmissivity curves of six one-strand sensors tested with 250-µm diameter Fluortex® ETFE deformer under contact.

Table 3. Correlation between displacements at coating fracture and transmissivity change of slope.

Test	In-Stack Net Displacement at Coating Fracture [µm]	In-Stack Net Displacement at Transmissivity Slope Change [µm]	Average Strain Rate [%/min]
FE-1	186	169	14.8
FE-2	170	190	13.4
FE-3	184	165	10.2
FE-4	172	171	10.7
F0-1	152	175	8.4
F0-3	186	184	12.3
Average	175	176	11.6
C.V.	7	5	19.9

The strain rate had little effect on the displacements at the light transmissivity drop (change of slope). In average, displacements recorded for sensors using Fluortex® ETFE deformers occurred at almost identical displacements to those predicted at coating fracture loads (between 35 and 45 N).

5. LOADING-UNLOADING-RELOADING TESTING

Since coating fracture would only occur during the first cycle (assuming that loads applied are larger than those expected to cause coating fracture), subsequent cycles may not present the slope change in the light transmissivity plots. To investigate if there were any changes in the transmissivity behavior observed after the first loading cycle, loading-unloading tests were conducted.

Because structures typically present different behaviors when comparing pre and post cracking conditions these tests were conducted at peak loads smaller and greater than the coating fracture loads determined by mechanical testing. Figure 5 presents four loading cycles to peak loads below coating fracture values.

After these four cycles, optical fiber and deformer were examined under the microscope. Glass-coating debonding was observed in the specimen. The deformer presented plastic deformations greater than those corresponding to the same load range observed previously. No cracks were observed on the optical fiber coatings.

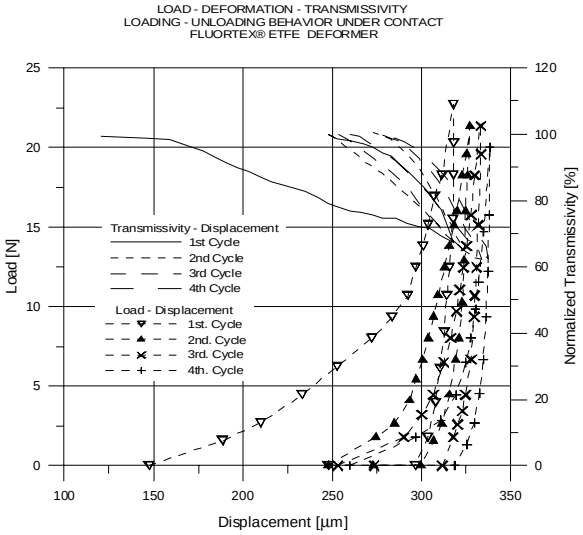

Figure 5. Typical loading-unloading curves for pre-coating fracture peak loads.

A marked difference between the first and the following cycles was observed. The virgin sample load-displacement curves enclosed a larger area than the subsequent loops. The energy dissipated during each cycle was determined by numerical integration and is presented in Table 4. Subsequent cycles show a decrement in irreversible deformations. Table 5 presents displacements registered for each type of behavior, i.e., elastic, viscoelastic and irreversible for each cycle.

Table 4. Summary of energy dissipated per loading-unloading cycle with a Fluortex® ETFE deformer: pre-cracking behavior.

Dissipated Energy [µJ]			
1st Cycle	2nd Cycle	3rd Cycle	4th Cycle
890	320	270	260

Table 5. Summary of displacements for loading-unloading cycles with a Fluortex® ETFE deformer: pre-cracking behavior.

Behavior	In-Stack Net Displacement [μm]			
	1st Cycle	2nd Cycle	3rd Cycle	4th Cycle
Irreversible	100	25	20	15
Elastic	21	21	22	20
Viscoelastic	49	35	38	43

Because of tolerance limitations in the measures of dissipated energy per cycle, cyclic testing was not conducted until constant dissipation energy values were attained. Figure 6 presents four loading-unloading cycles to peak loads greater than coating fracture loads.

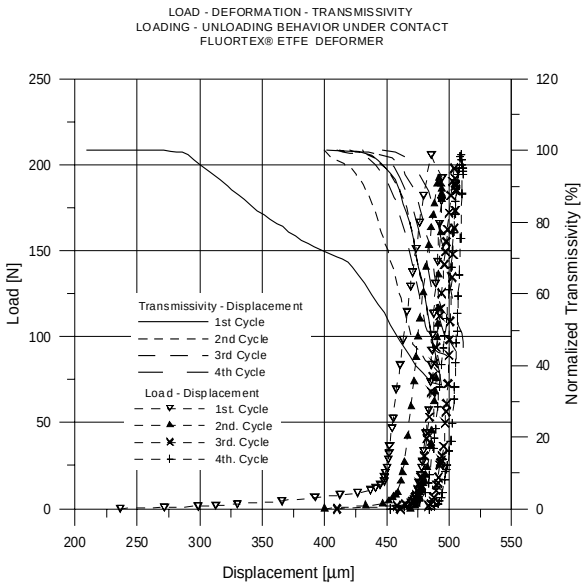

Figure 6. Typical loading-unloading curves for post-coating fracture peak loads.

The light transmissivity change of slope observed during the optical performance testing phase was present in the first loading-unloading cycle (Figure 6) but not in the subsequent cycles. This is because the coating fracture is a one-time event; therefore subsequent cycles do not present the previously observed slope change in the light transmissivity curves. Again, the energy dissipated during each cycle was determined by numerical integration and is presented in Table 6. Table 7 presents displacements registered for elastic, viscoelastic and irreversible behaviors for each cycle.

Table 6. Summary of energy dissipated per loading-unloading cycle with a Fluortex® ETFE deformer: post-cracking behavior.

Dissipated Energy [μJ]			
1st Cycle	2nd Cycle	3rd Cycle	4th Cycle
5,600	2,800	2,000	1,900

Table 7. Summary of displacements for loading-unloading cycles with a Fluortex® ETFE deformer: post-cracking behavior.

Behavior	In-Stack Net Displacement [μm]			
	1st Cycle	2nd Cycle	3rd Cycle	4th Cycle
Irreversible	121	32	27	21
Elastic	37	36	35	35
Viscoelastic	55	51	45	45

Throughout loading-unloading testing, it was observed that irreversible deformations decrease with increasing number of cycles. Sensors dissipated a noticeably larger energy during the first cycle than all subsequent cycles for pre and post coating fracture conditions. It was also observed that after the first cycle, the light transmissivity-displacement curve becomes more linear and yields more consistent output results. It is believed by the authors that for pre-cracking peak loads the larger energy dissipated during the first cycle is caused by debonding.

6. FINITE ELEMENT ANALYSIS

A Finite Element Analysis was performed to determine if the coating fracture loads measured during the experimental phase could be correlated to strength properties reported. Mechanica® (release 2001) was the code chosen for this analysis based on availability. Relatively simple three-dimensional Finite Element models were employed (Figure 7). Finite Element code limitations included modeling of elastic-viscoplastic behavior of polymers, crushing and crack propagation. Capabilities for simulating strain rate-dependent materials such as polymers and acrylate-like materials were also absent.

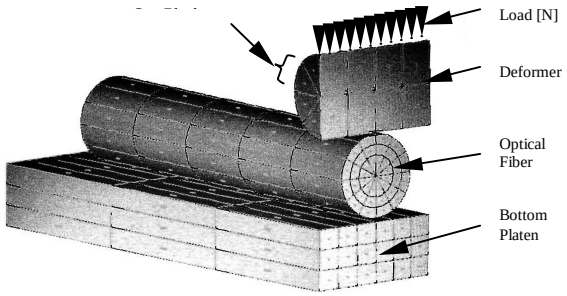

Figure 7. Three-dimensional Finite Element Mesh.

The Octahedral Shear Stress Yield was the adopted coating failure criterion. Result from the models showed that maximum stresses were developed at the inner surface of the secondary coating. Other important stresses were those developed at the contact region. Model results were plotted as load-stress and displacement-stress curves to assist in correlating model results to experimental results. Figures 8 and 9 show these curves.

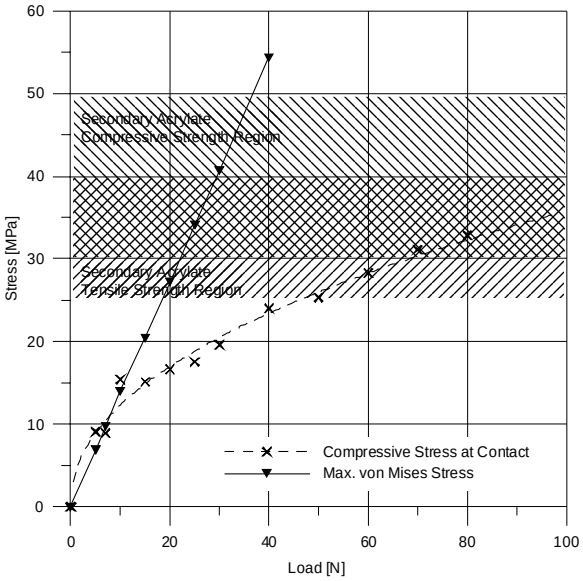

Figure 8. Finite Element load-stress results.

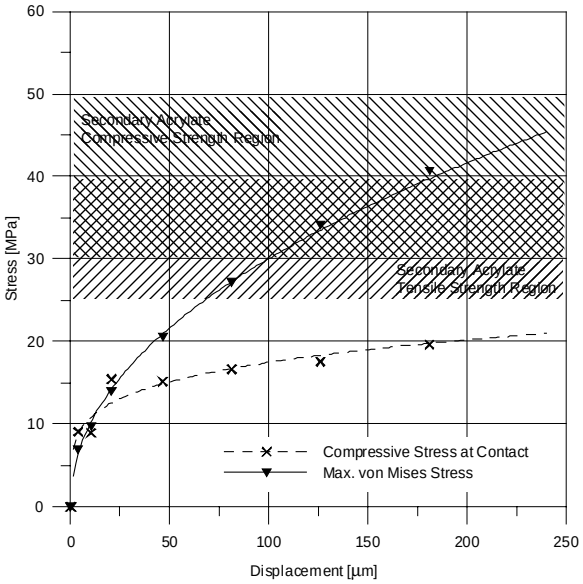

Figure 9. Finite Element displacement-stress results.

Loads and displacements predicted by the Finite Element models were similar to those observed experimentally when using the maximum reported coating tensile strength (40 MPa). Table 8 summarizes experimental and numerical models results.

Table 8. Summary of Corning® 50/125/250 secondary coating failure loads and displacements under one-sided microbend contact with a Fluortex® ETFE deformer.

Strength Parameter	Load [N]	Displacement [μm]
Experimental Analyses		
Coating Failure	≅ 35 to 45	152 to 186
Finite Element Analyses		
Min. Strength (25 MPa)	≅ 18	≅ 74
Max. Strength (40 MPa)	≅ 30	≅ 178

Despite the limitations of the Finite Element code employed, the results obtained were in agreement with those recorded during experimental analyses. The predicted stresses developed within the optical fiber for the loads observed to cause coating fracture were correlated to reported coating strength values falling within 15% while the displacements predicted by the models fell within 2% of the average displacements recorded experimentally.

7. CONCLUSIONS

During experimental analyses two damage mechanisms were identified: glass-coating debonding and coating fracture. Glass-coating debonding begun at loads of approximately 10±3 N and coating fracture occurred at loads between 35 and 45 N. Coating fracture allowed direct contact between deformer and optical fiber glass (core and cladding) resulting in a distinctive change of slope in the light transmissivity curves when using Fluortex® ETFE deformers in virgin sensors.

Fluortex® ETFE sensors output presented little variation with respect to strain rate changes, for the strain rates tested during this research (sensors constructed using stiffer deformers presented a higher sensitivity to strain rate).

During loading-unloading events, it was observed that irreversible deformations decreased with increasing number of cycles. A noticeably larger energy was dissipated during the first cycle than all subsequent cycles for pre and post coating fracture conditions. After the first cycle, the light transmissivity-displacement curve became more linear and yielded more consistent output results. Because of the variations in the sensor's output during the first few cycles due to irreversible processes, a need for mechanical conditioning was established. In all cases, light transmissivity was fully recovered after removing the load, i.e., glass fracture did not occur.

It was found that relatively simple three-dimensional Finite Element models are able to predict coating fracture with acceptable tolerance. Maximum predicted stresses were located at the inner face of the secondary coating. Because of this, it is presumed that cracks in the secondary coating are generated at the inner surface and propagate outward. Because it is believed that damage mechanisms (such as surface cracks and coating fracture) can reduce the service life and affect the performance of the optical fiber, it is recommended that the loads per contact point are kept below the fracture values determined in this research (35 to 45N) when using deformers with comparable mechanical properties.

Tests using stiffer deformers presented strain rate sensitivity. To avoid output variations because of strain rate sensitivity it is recommended to use lower stiffness deformers.

During sensor calibration, it is recommended to discard the set of data corresponding to the first few loading-unloading cycles because of the scatter that is introduced in the sensors' output. Sensors should be subjected to mechanical conditioning before calibration and service.

8. REFERENCES

[1] Campero, F., 2004 “Analysis of the Failure Characteristics of the Optical Fiber Coating in Fiber Optic Microbend Sensors”, UMI Press, Ann Arbor, MI (ISBN # 0-493-55035-6).

[2] Glaesemann, G.S., 1999, “Advancements in Mechanical Strength and Reliability of Optical Fibers”, SPIE Proceedings, Boston, MA, Vol. CR73.

[3] Cosentino, P.J., Campero, F. and Lloyd, P.B., 2002, “Developing Geotechnical Applications for the Fiber Optic Pore Water Pressure Sensor Phase I”, Final Report, FDOT, Contract Number BC 796, Melbourne, Florida.